

# OPTIMAL 3D ORBIT CORRECTIONS IN CURVILINEAR COORDINATES

Juan L. Gonzalo\*, and Claudio Bombardelli†

The minimum-time, constant-thrust orbit correction between two close non-coplanar circular orbits is studied using a relative motion formulation in curvilinear coordinates. The associated optimal control problem in the thrust orientation is tackled using the direct method to numerically solve a diverse set of problems for varying orbital radius and inclination. Additionally, an analytical estimate for the minimum-time inclination change maneuver is obtained. Fundamental changes in the structure of the solution and objective function are highlighted depending on the relation between the required radial displacement, inclination change and available thrust.

## INTRODUCTION

The increasing concern about space debris accumulation has led to the proposal of a wide variety of Active Debris Removal missions. While substantial differences appear in the physical principles used to manipulate the target debris (contactless manipulation using ion beams or gravity tractors, mechanical coupling with robotic arms, nets or harpoons, etc), most of them share the need to perform a precise rendezvous or docking maneuver with the non-cooperative and normally not completely characterized target debris. A particular example of such a mission is provided by LEOSWEEP (improving LEO Security With Enhanced Electric Propulsion),<sup>1</sup> an EU-funded project aiming at the contactless manipulation of non-cooperative targets using modified electric thrusters. The base LEOSWEEP mission would not only require to transfer from the original orbit, be it the injection one or the final state from a previous debris removal, but also to continuously correct the relative position between debris and satellite. Other key missions also require precise orbit corrections, such as cooperative rendezvous and docking maneuvers, fundamental for the operation of the ISS, and those involving formation flying of satellites.

The practical interest of this family of maneuvers is reflected in the attention they have received in the last decades. A detailed analytical study on the subject, including closed form solutions for some particular conditions, can be found in the book by Marec.<sup>2</sup> A classification of the different regimes for the phasing problem was performed by Hall and Collazo-Perez<sup>3</sup> using numerical techniques. More recently, the authors of the present work have considered both analytical and numerical techniques to analyze the planar phasing<sup>4</sup> and radius change<sup>5</sup> maneuvers using relative motion formulations. The combination of analytical and numerical approaches has proven to be synergistic: while it is not possible to fully solve the problem using the former, it provides the physical insight to fully characterize the different regimes observed with the latter. Furthermore,

---

\*PhD candidate, Space Dynamics Group, School of Aerospace Engineering, Technical University of Madrid (UPM).

†Research Associate, Space Dynamics Group, School of Aerospace Engineering, Technical University of Madrid (UPM).

it also serves as a means to construct approximate solutions useful for estimation or initial guess generation.

This work deals with the minimum-time orbit correction between two close, non-coplanar, circular orbits, assuming continuous thrust and using a non-linear relative motion formulation for the dynamics.<sup>6</sup> It can be seen as the finalization of the previous works on the phasing and radius change problems,<sup>4,5</sup> and as such it has a special focus on the out-of-plane component of the motion. The formulation used to describe the dynamics yields a very compact set of equations using as variables the radial separation, the phasing and the out-of-plane distance, and proves to be very convenient for both the numerical and analytical analysis. Compared to the well-known Clohessy-Wiltshire equations,<sup>7</sup> it has the advantages of better describing the orbit curvature and providing a more accurate solution through the inclusion of non-linear terms.

The optimal control problem in the thrust orientation is treated numerically but starting from key analytical relations to support the generation of a suitable initial guess. The first analytical relation is concerned with the minimum-time change of inclination with unaltered orbit radius. An exact optimal solution in closed analytical form is obtained starting from the linearized equations of motion and therefore is valid for small inclination changes. The solution is employed to generate the initial guess for a sequence of optimization problems in which a gradual change in orbit radius is imposed together with the fixed inclination change. The second analytical relation is concerned with the minimum-time change of orbital radius and was obtained in a previous work by the authors.<sup>5</sup> The structure of the solution when going from an inclination-only problem towards an increasingly radial-change-characterized problem is studied with an emphasis on the evolution of the minimum maneuver time. The relation between the latter and the sum of the maneuver times required for the inclination-only and radial-only subproblems is investigated.

## PROBLEM STATEMENT AND EQUATIONS OF MOTION

The objective is to study the minimum-time orbit corrections between two close, non-coplanar orbits. In the more general case, this implies modifying the radius, the inclination and the phasing of the orbit. To model the problem, let us consider two objects, a leader  $L$  and a chaser  $C$ , describing two close circular orbits of radii  $R$  and  $R_C$  around a primary  $O$  with gravitational constant  $\mu$ . The chaser is the controllable spacecraft whose orbit will be modified, and the leader may represent a real object (e.g. another spacecraft, a space debris) or a virtual one (such as the nominal final position of the spacecraft). All the equations and variables will be expressed in non-dimensional form, taking the following characteristic magnitudes for length, time and mass:

$$R, \quad \Omega^{-1} = \sqrt{\frac{R^3}{\mu}}, \quad m_C,$$

where  $m_C$  is the mass of the chaser. Since we are studying small orbit modifications the required propellant mass  $m_{\text{prop}}$  can be assumed to be negligible compared to  $m_C$ , and the latter is taken as constant.

Dynamics will be described using the non-linear relative motion formulation in curvilinear coordinates recently proposed by Bombardelli et al.<sup>6</sup> Let us begin by introducing a Local Vertical-Local Horizontal (LVLH) reference frame centered at the leader  $\mathcal{F} = \{L; \mathbf{i}', \mathbf{j}', \mathbf{k}'\}$ . The cartesian position and velocity of the follower take the form:

$$\mathbf{r} = x\mathbf{i}' + y\mathbf{j}' + z\mathbf{k}', \quad \mathbf{v} = \dot{x}\mathbf{i}' + \dot{y}\mathbf{j}' + \dot{z}\mathbf{k}'.$$

The in-plane coordinates  $x$  and  $y$  can be replaced by two curvilinear coordinates  $\theta$ , the angle formed by the position vectors of chaser and leader, and  $\rho$ , the radial separation of the chaser from the orbit of the leader. These coordinates are related as follows:

$$\begin{aligned}\rho &= -1 + \sqrt{(x+1)^2 + y^2}, & \theta &= \text{atan2}(y, 1+x), \\ x &= -1 + (1+\rho)\cos\theta, & y &= (1+\rho)\sin\theta.\end{aligned}$$

Projecting the equations of motion along the radial, transversal and normal unity vectors

$$\mathbf{u}_\rho = \cos\theta\mathbf{i}' + \sin\theta\mathbf{j}', \quad \mathbf{u}_\theta = -\sin\theta\mathbf{i}' + \cos\theta\mathbf{j}', \quad \mathbf{u}_z = \mathbf{k}',$$

one finally reaches:

$$\begin{aligned}\ddot{\rho} - 2\dot{\theta} - 3\rho &= a_{i\rho} + a_{g\rho} + a_\rho^T \\ \ddot{\theta} + 2\dot{\rho} &= a_{i\theta} + a_\theta^T \\ \ddot{z} + z &= a_{gz} + a_z^T\end{aligned}\tag{1}$$

where  $a_{i\rho}$ ,  $a_{g\rho}$ ,  $a_{i\theta}$  and  $a_{gz}$  account for the non-linear perturbation terms

$$\begin{aligned}a_{i\rho} &= \dot{\theta}^2(1+\rho) + 2\dot{\theta}\dot{\rho}, & a_{i\theta} &= \frac{2\dot{\rho}(\rho - \dot{\theta})}{1+\rho}, \\ a_{g\rho} &= -2\rho + 1 - \frac{1+\rho}{\left[(1+\rho)^2 + z^2\right]^{3/2}}, & a_{gz} &= z - \frac{z}{\left[(1+\rho)^2 + z^2\right]^{3/2}},\end{aligned}$$

while  $a_\rho^T$ ,  $a_\theta^T$  and  $a_z^T$  correspond to the actions of the continuous-thrust engine. The thruster's acceleration can also be expressed through the total magnitude of the acceleration  $a^T$  and a unitary vector  $\mathbf{u}^T$ :

$$\begin{aligned}a^T &= \sqrt{(a_\rho^T)^2 + (a_\theta^T)^2 + (a_z^T)^2}, & \mathbf{u}^T &= \left[ u_\rho^T \quad u_\theta^T \quad u_z^T \right]^T, \quad \|\mathbf{u}^T\| = 1, \\ a_\rho^T &= a^T u_\rho^T, & a_\theta^T &= a^T u_\theta^T, & a_z^T &= a^T u_z^T.\end{aligned}$$

Although this representation of control is redundant, introducing one additional variable and an algebraic restriction, it will be preferred for the numerical treatment of the problem due to its better behavior for small values of  $a^T$ .

Introducing the state vector

$$\mathbf{S} = \left[ \dot{\rho} \quad \dot{\theta} \quad \dot{z} \quad \rho \quad \theta \quad z \right]^T,$$

and the control vector

$$\mathbf{U} = \left[ u_\rho^T \quad u_\theta^T \quad u_z^T \quad a^T \right]^T,$$

Eqs. (1) can be reduced to the first order system:

$$\frac{d\mathbf{S}}{d\tau} = \mathbf{F}(\tau, \mathbf{S}; \mathbf{U}), \quad \text{with} \quad \mathbf{F}(\tau, \mathbf{S}; \mathbf{U}) = \begin{bmatrix} 2\dot{\theta} + 3\rho + a_{i\rho} + a_{g\rho} + a^T u_\rho^T \\ -2\dot{\rho} + a_{i\theta} + a^T u_\theta^T \\ -z + a_{gz} + a^T u_z^T \\ \dot{\rho} \\ \dot{\theta} \\ \dot{z} \end{bmatrix}, \tag{2}$$

where  $\tau$  is the non-dimensional time. An additional equation must be imposed to the components of the control vector to reflect the physical limit of the maximum available thrust, depending on the representation used for control either

$$0 < a^T < \varepsilon, \quad (3)$$

or

$$(a_\rho^T)^2 + (a_\theta^T)^2 + (a_z^T)^2 \leq \varepsilon^2,$$

where  $\varepsilon$  is the non-dimensional nominal thruster acceleration

$$\varepsilon = \frac{T}{m_C R \Omega^2}$$

being  $T$  the nominal thrust. The linearized formulation, used in some parts of the study, is similar to the well-known Clohessy-Wilshire equations:

$$\frac{d\mathbf{S}}{d\tau} = \mathbf{F}^*(\tau, \mathbf{S}; \mathbf{U}), \quad \text{with} \quad \mathbf{F}^*(\tau, \mathbf{S}; \mathbf{U}) = \begin{bmatrix} 2\dot{\theta} + 3\rho + a^T u_\rho^T \\ -2\dot{\rho} + a^T u_\theta^T \\ -z + a^T u_z^T \\ \dot{\rho} \\ \dot{\theta} \\ \dot{z} \end{bmatrix}. \quad (4)$$

It is important to note that the only coupling between the in-plane and out-of-plane linearized equations comes from the thrust restriction expressed through Eq. (3).

The final state of the chaser is determined from the state of the leader. In general, one can consider any arbitrary phasing  $\Delta\theta$  between leader and chaser in the final state, but the values of  $\rho$ ,  $z$  and all the derivatives should be zero so that the orbits of chaser and leader coincide:

$$\mathbf{S}(\tau_f) = \begin{bmatrix} \dot{\rho}_f & \dot{\theta}_f & \dot{z}_f & \rho_f & \theta_f & z_f \end{bmatrix}^\top = \begin{bmatrix} 0 & 0 & 0 & 0 & \Delta\theta & 0 \end{bmatrix}^\top. \quad (5)$$

The initial state corresponds to the original orbit of the chaser. Said orbit can be characterized by three parameters: its inclination with respect to the leader orbit  $\Delta i$ , the difference in radius with respect to the leader orbit  $\Delta r = (R - R_C)/R$ , and the time since the chaser crossed the orbit plane of the leader at the ascending node  $\tau_0$ . Note that the sign of  $\Delta r$  indicates whether the initial orbit is above the reference orbit, negative  $\Delta r$ , or below it, positive  $\Delta r$ . An additional simplification has been made in the equations by imposing that the leader is placed along the line of nodes at  $\tau_0$ ; this can be done without loss of generality by defining a new virtual leader and including its phasing with respect to the real one as part of  $\theta_f$ . From these parameters, the initial state can be computed as:

$$\mathbf{S}(\tau_0) = \begin{bmatrix} \dot{\rho}_0 & \dot{\theta}_0 & \dot{z}_0 & \rho_0 & \theta_0 & z_0 \end{bmatrix}^\top, \quad (6)$$

with:

$$\dot{\rho}_0 = \frac{\kappa \sin(2n_0\tau_0)}{2\sqrt{(1 - \Delta\rho)[1 - \kappa \sin^2(n_0\tau_0)]}},$$

$$\dot{\theta}_0 = -1 + \frac{n_0\sqrt{1 - \kappa}}{(1 - \kappa)\sin^2(n_0\tau_0) + \cos^2(n_0\tau_0)},$$

$$\begin{aligned}\dot{z}_0 &= \frac{\sqrt{\kappa} \cos(n_0 \tau_0)}{\sqrt{1 - \Delta r}}, \\ \rho_0 &= -1 + (1 - \Delta r) \sqrt{1 - \kappa \sin^2(n_0 \tau_0)}, \\ \theta_0 &= -\tau_0 + \text{atan2}(\sqrt{1 - \kappa} \sin(n_0 \tau_0), \cos(n_0 \tau_0)), \\ z_0 &= (1 - \Delta r) \sqrt{\kappa} \sin(n_0 \tau_0),\end{aligned}$$

where:

$$\kappa = \sin^2 \Delta i, \quad n_0 = \frac{1}{\sqrt{(1 - \Delta r)^3}}.$$

## INCLINATION CHANGE SUBPROBLEM

When  $\Delta r = 0$  and no phasing is imposed the only orbit correction to be performed is an inclination change. However, the coupling between Eqs. (2) and the dependence of  $\dot{\rho}_0$ ,  $\dot{\theta}_0$ ,  $\rho_0$  and  $\theta_0$  with  $\Delta i$  implies that some degree of in-plane control will be needed even in this simplified maneuver. In cases where  $\Delta i$  is small the linearized model given by Eqs. (4) can be used, uncoupling the in-plane and out-of-plane equations; the only coupling then comes from the maximum thrust restriction. Relaxing this condition (i.e. neglecting the in-plane thrust requirements), the out-of-plane dynamics in the linear approximation is described as:

$$\begin{aligned}\ddot{z} + z &= a_z^T, \\ |a_z^T| &\leq \varepsilon,\end{aligned}\tag{7}$$

with initial conditions at  $0 < \tau_0 < 2\pi$ :

$$\begin{aligned}z(\tau_0) &= z_0 = \sqrt{\kappa} \sin \tau_0, \\ \dot{z}(\tau_0) &= \dot{z}_0 = \sqrt{\kappa} \cos \tau_0.\end{aligned}$$

Note that Eq. (7) corresponds to a forced linear oscillator. The minimum-time strategy to drive the out-of-plane velocity to zero is to have:

$$a_z^T = -\varepsilon \text{sign}(\dot{z}),$$

but in general this does not assure that  $z$  will also reach zero along with  $\dot{z}$ . Nevertheless, it is possible to force this condition by choosing an adequate time  $\tau_0$  to start the maneuver.

The solution of Eq. (7) for the proposed control between the initial time  $\tau_0$  and the first control switch (zero velocity) time  $\tau_1$  is:

$$\begin{aligned}z(\tau_0 < \tau < \tau_1) &= \dot{z}_0 \sin(\tau - \tau_0) + (z_0 - \varepsilon) \cos(\tau - \tau_0) - \varepsilon, \\ \dot{z}(\tau_0 < \tau < \tau_1) &= \dot{z}_0 \cos(\tau - \tau_0) - (z_0 - \varepsilon) \sin(\tau - \tau_0),\end{aligned}$$

where the switching time  $\tau_1$  obeys:

$$\tau_1 - \tau_0 = \begin{cases} \tau^* & \text{for } \dot{z}_0 (z_0 - \varepsilon) > 0 \\ \pi/2 & \text{for } z_0 = \varepsilon \\ \tau^* + \pi & \text{for } \dot{z}_0 (z_0 - \varepsilon) < 0 \end{cases}$$

$$\tau^* = \text{atan} \left( \frac{\dot{z}_0}{z_0 - \varepsilon} \right),$$

and the coordinate at the switching point reads:

$$z_1 = z(\tau_1) = \varepsilon \pm \sqrt{\dot{z}_0^2 + (z_0 - \varepsilon)^2},$$

where the positive sign corresponds to the case  $\dot{z}_0(z_0 - \varepsilon) > 0$ .

For the successive sections between consecutive switching points ( $n = 2, \dots, N$ ) the solution is:

$$\begin{aligned} z_n(\tau_{n-1} < \tau < \tau_n) = \\ = -\varepsilon \pm \frac{[\dot{z}_0 \sin(\tau - \tau_0) + (z_0 - \varepsilon) \cos(\tau - \tau_0)] \left[ \pm \sqrt{\dot{z}_0^2 + (z_0 - \varepsilon)^2} + (-1)^n (2n - 1) \varepsilon \right]}{\sqrt{\dot{z}_0^2 + (z_0 - \varepsilon)^2}}, \end{aligned}$$

with:

$$\tau_n = \tau_1 + (n - 1) \pi,$$

and:

$$z_n = z(\tau_n) = (-1)^n \left[ -(2n - 1) \varepsilon \mp \sqrt{\dot{z}_0^2 + (z_0 - \varepsilon)^2} \right].$$

By imposing  $z_n = 0$  one can now derive the optimum maneuver start time  $\tau_0$  to have the forced oscillator arrive at  $z = 0$  with zero velocity:

$$\sin \tau_0 = - \left[ \frac{2N(N - 1)}{\Theta} - \frac{\Theta}{2} \right], \quad \cos \tau_0 = -\sqrt{1 - \sin^2 \tau_0}, \quad (8)$$

where

$$\Theta = \frac{\sin \Delta i}{\varepsilon} > 0, \quad (9)$$

is a non-dimensional parameter quantifying the duration of the inclination change maneuver. The total number of required cycles is:

$$N = 1 + \left\lfloor \frac{\Theta}{2} \right\rfloor,$$

where  $\lfloor \cdot \rfloor$  represents the floor operator, and the total maneuver time finally yields:

$$\Delta \tau = \pi(N - 1) + \tau_1 - \tau_0 = \pi \left\lfloor \frac{\Theta}{2} \right\rfloor + \tau_1 - \tau_0. \quad (10)$$

From the definition of  $\tau_1 - \tau_0$  it is straightforward to check that its value is bounded and always lies between 0 and  $\pi$ . Consequently, for  $\Theta < 2$  the required maneuver time equals  $\tau_1 - \tau_0$ , while for  $\Theta \gg 1$  it mainly depends on  $\Theta$ . It is key to highlight that  $\Theta$  represents the ratio between the desired displacement and the available thrust. For a small inclination variation  $\Delta i$  it is possible to write Eq. (10) as:

$$\Delta \tau \simeq \pi \left\lfloor \frac{\Delta i}{2\varepsilon} \right\rfloor + \tau_1 - \tau_0.$$

This behavior shows important qualitative similarities with the same-orbit rephasing and the planar radius change orbit corrections already studied by these authors.<sup>4,5</sup> In both cases, simple expressions for the time of flight as a function of the ratio between the desired displacement and the available thrust parameter were found, using the linearized equations of relative motion and the Euler-Lagrange first order optimality conditions. For the phasing problem, two different regimes were found:

$$\Delta\tau \simeq \sqrt{\frac{4}{3}} \frac{|\Delta\theta|}{\varepsilon} \quad \text{for } |\Delta\theta| \gg \varepsilon,$$

$$\Delta\tau \simeq 2\sqrt{\frac{|\Delta\theta|}{\varepsilon}} \quad \text{for } |\Delta\theta| \ll \varepsilon,$$

and also for the radius change maneuver:

$$\Delta\tau \simeq \frac{|\Delta r|}{2\varepsilon} \quad \text{for } |\Delta r| \gg \varepsilon,$$

$$\Delta\tau \simeq 2\sqrt{\frac{|\Delta r|}{\varepsilon}} \quad \text{for } |\Delta r| \ll \varepsilon.$$

The key difference between both regimes was whether the maneuver could be completed within one orbit or not. Furthermore, the corresponding structures of the control law and the evolution of the state also showed fundamental qualitative differences between regimes. In the inclination change subproblem there is no qualitative change in the control profile between both regimes, but the main contribution to the maneuver time switches from  $\tau_1 - \tau_0$  in the less-than-one-orbit case to  $\pi[\Theta/2]$  in the multiple-revolutions scenario.

These approximate solutions for the radius-only, phasing-only and inclination-only problems can be used to generate reasonably accurate initial estimations of a maneuver. For any given case, the profile corresponding to the most time-demanding individual subproblem should be used as a base. Since  $\varepsilon$  is the same for all the expressions, this provides a decision criterion based on the relative values of  $\Delta i$ ,  $\Delta r$  and  $\Delta\theta$ . Furthermore, a fast estimate for the time of flight can be obtained by adding the  $\Delta\tau$  estimates for each individual maneuver; the results in the following section will show that this estimate is conservative.

## NUMERICAL SOLUTION WITH DIRECT METHODS

The proposed minimum-time orbit correction between two close, non-coplanar, circular orbits is now solved numerically for the continuous, limited thrust case, using a direct transcription method.<sup>8,9</sup> While the control is not restricted to constant thrust, the results show that it will naturally tend to use all the available thrust as it is common with minimum-time problems. Furthermore, since the mass of the maneuvering spacecraft has been assumed to be constant this problem is equivalent to minimizing the total impulse for the transfer.

The optimal control problem (OCP) will be solved for several values of inclination and radial displacement. While the algorithm also allows for a fixed value of  $\theta$ , in order to better study the interaction between radius and inclination change the final phasing will be set free:

$$-\infty < \theta_f < \infty.$$

For simplicity the initial time  $\tau_0$  will be fixed, taking the value which optimizes the inclination-only linearized subproblem, Eqs. (8).

In order to transcribe the original, continuous problem into a discrete Non-Linear Programming (NLP) one the trapezoidal discretization and a uniformly spaced grid of  $M$  nodes are used. The optimization variable  $\mathbf{x}$  is then formed by the values of state  $\mathbf{S}$  and control  $\mathbf{U}$  at each node of the grid, together with the free final time  $\tau_f$ . The grid is constructed using a normalized ‘time’ variable  $t$  defined in the range  $[0, 1]$ , so the physical non-dimensional time can be expressed as  $\tau = \tau_0 + t(\tau_f - \tau_0)$ . This allows for the node positions in  $t$  to be constant while  $\tau_f$  varies as part of the optimization variable. Furthermore, the objective function  $J$  simply takes the form:

$$J = \tau_f - \tau_0,$$

where  $\tau_0$  is constant.

The equations of motion, Eqs. (2), are expressed as a set of non-linear equality constraints called *defect constraints* using the Trapezoidal Method, a 2-stages, 3<sup>rd</sup> order Implicit Runge-Kutta scheme. The selection of an IRK algorithm is based on their good performance for this kind of applications.<sup>8,10</sup> This yields a total of  $6(M - 1)$  defect constraints, each one involving only two adjacent nodes. An additional set of non-linear equality constraints results from imposing the thrust orientation vector  $\mathbf{u}^T$  to be unitary, producing  $M$  extra equations each one involving the three components of  $\mathbf{u}^T$  at the corresponding node. The Jacobian for these defect and control constraints is constructed analytically, exploiting its strong sparsity. Since each defect constraint only depends on  $\tau_f$  and two neighboring nodes, and each control constraint only on one, an adequate ordering of the constraints and the optimization variable allows to place all the non-zero elements of the Jacobian either in the first column or in a narrow band along the main diagonal. The constraints for the OCP are finally completed with the simple bound constraints coming from the known values of the state at  $\tau_0$  and  $\tau_f$ , Eqs. (6) and (5) respectively, and the maximum nominal value for the thrust acceleration, Eq. (3).

The NLP subproblem is solved numerically using *Ipopt* (Interior Point OPTimizer), a third-party software package for large-scale nonlinear optimization.<sup>11</sup> It is distributed as open source code under the Eclipse Public License (EPL), and available from the COIN-OR initiative\*. The analytical expressions for the objective function, the non-linear constraints and their corresponding derivatives are fed to the algorithm as required inputs, while a choice is made for the Hessian. For small grids ( $M < 300$ ) a user-supplied Hessian is calculated numerically using finite differences of the gradients,<sup>12</sup> while the build-in L-BFGS update is preferred for larger grids. This decision is based on computational cost considerations: although the former way of computing the Hessian is more precise, requiring a smaller number of iterations to converge, the approximation given by the latter is faster to compute and factorize. From a computational cost point of view the advantages of the L-BFGS update outweigh those of the finite differences approximation as the number of nodes increases, justifying a change in strategy.

The proposed transcription is probably one of the simplest that can be considered for numerically solving an OCP using direct methods. Although this could be seen as a drawback at first, it is actually an advantage for this study. On the one hand, the focus is in the use of a new formulation for dynamics and the characterization of the maneuver, not the transcription itself. On the other hand, the good results obtained using a simple method seem to indicate that further advantages could be obtained in the future by considering more elaborated transcriptions.

The minimum-time transfer is now computed for several values of the inclination  $\Delta i$ , the radial

---

\*<http://www.coin-or.org/>



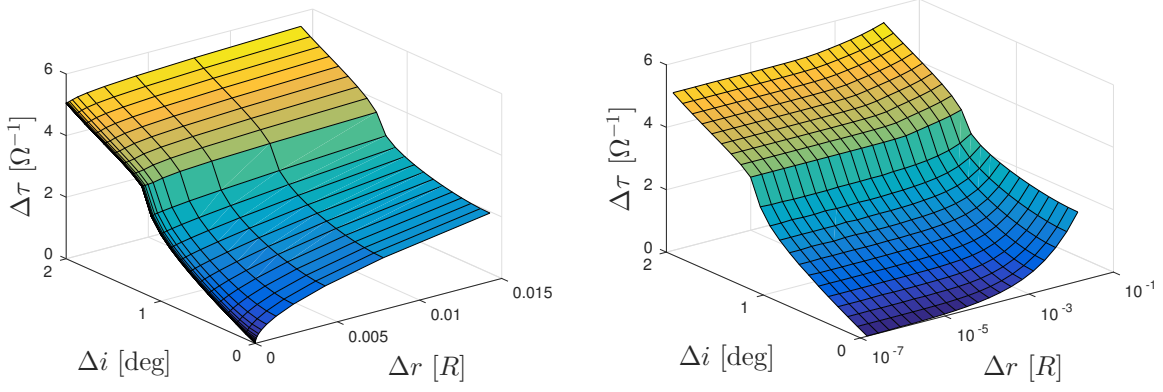


**Figure 1. Time of flight as a function of the radial displacement and the inclination change for a non-dimensional thrust parameter of 0.01.**

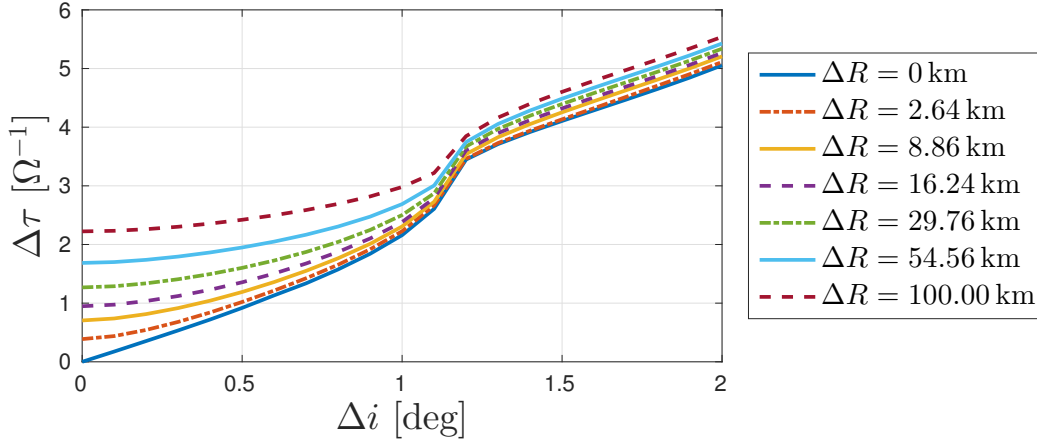


**Figure 2. Time of flight as a function of the inclination change for several radial displacements and a non-dimensional thrust parameter of 0.01.**

displacement  $\Delta r$  and the thrust parameter  $\varepsilon$ . In all cases the final, or reference, orbit is defined as

$$R = 7000 \text{ km}, \quad T_{\text{orb}} = 97.142 \text{ min}, \quad \Omega = 1.078 \cdot 10^{-3} \text{ rad/s},$$

where  $T_{\text{orb}}$  is the orbital period of said orbit. Several inclinations between 0 and 2 degrees are considered, while the radial displacement varies in the 0 to 100000 meters range (corresponding to  $0 \leq \Delta r \leq 1.429 \cdot 10^{-2}$ ). The NLP problem is solved iteratively, starting with a fast approximation computed for a coarse grid (50 to 300 nodes) and an initial guess constructed from the analytical results previously presented. This first approximation is then used as initial guess for a finer grid, and the process continues until an accurate enough optimum is obtained.

Figures 1-4 show the results obtained for a thrust parameter of  $\varepsilon = 10^{-2}$ , which corresponds to a thrust acceleration of one hundred of the local gravity at the final orbit (for a 1 kg spacecraft, this amounts to 81.35 mN). While this value is high from a physical point of view, so are the required displacements in inclination and radius. In all cases, this allows to perform the maneuver within one orbital revolution. The time of flight as a function of the radial displacement and the inclination change is represented in Figures 1-3. Considering the evolution of  $\Delta\tau$  with  $\Delta r$  first, Figure 3, it is observed that the slope with  $\Delta r$  decreases as  $\Delta i$  increases. Likewise, Figure 2 reveals

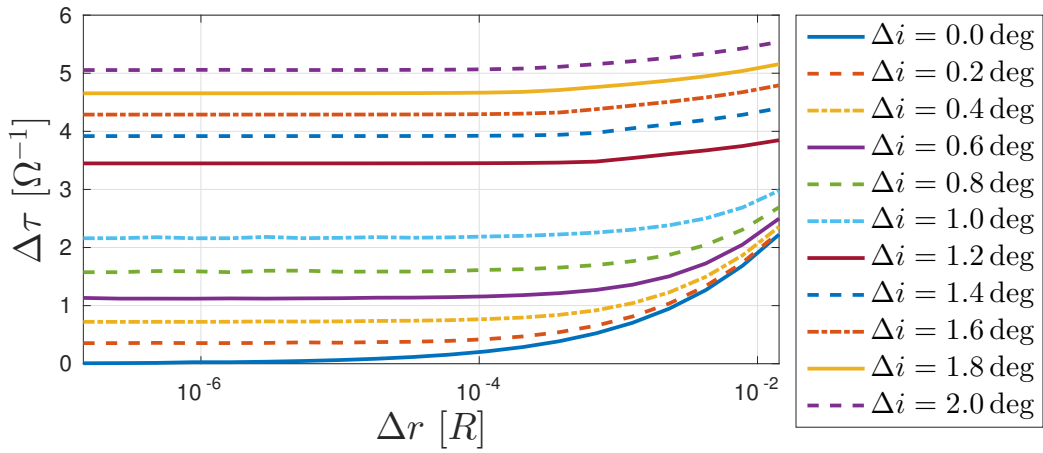


**Figure 3. Time of flight as a function of the radial displacement for several inclination changes and a non-dimensional thrust parameter of 0.01.**

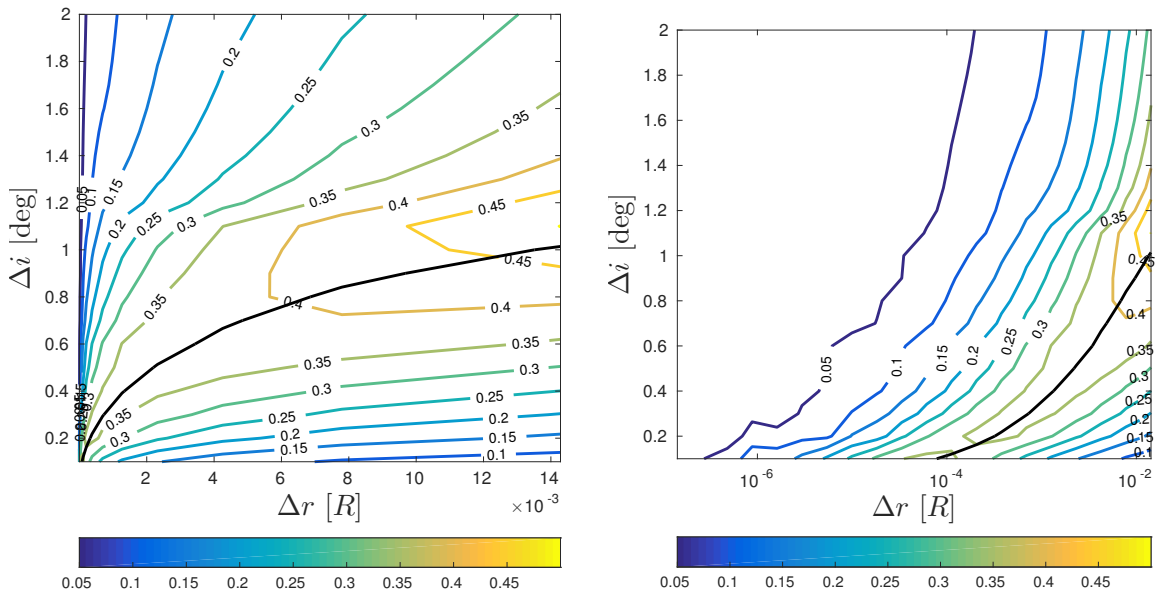


**Figure 4. Synergy coefficient as a function of the radial displacement and the inclination change for a non-dimensional thrust parameter of 0.01.**

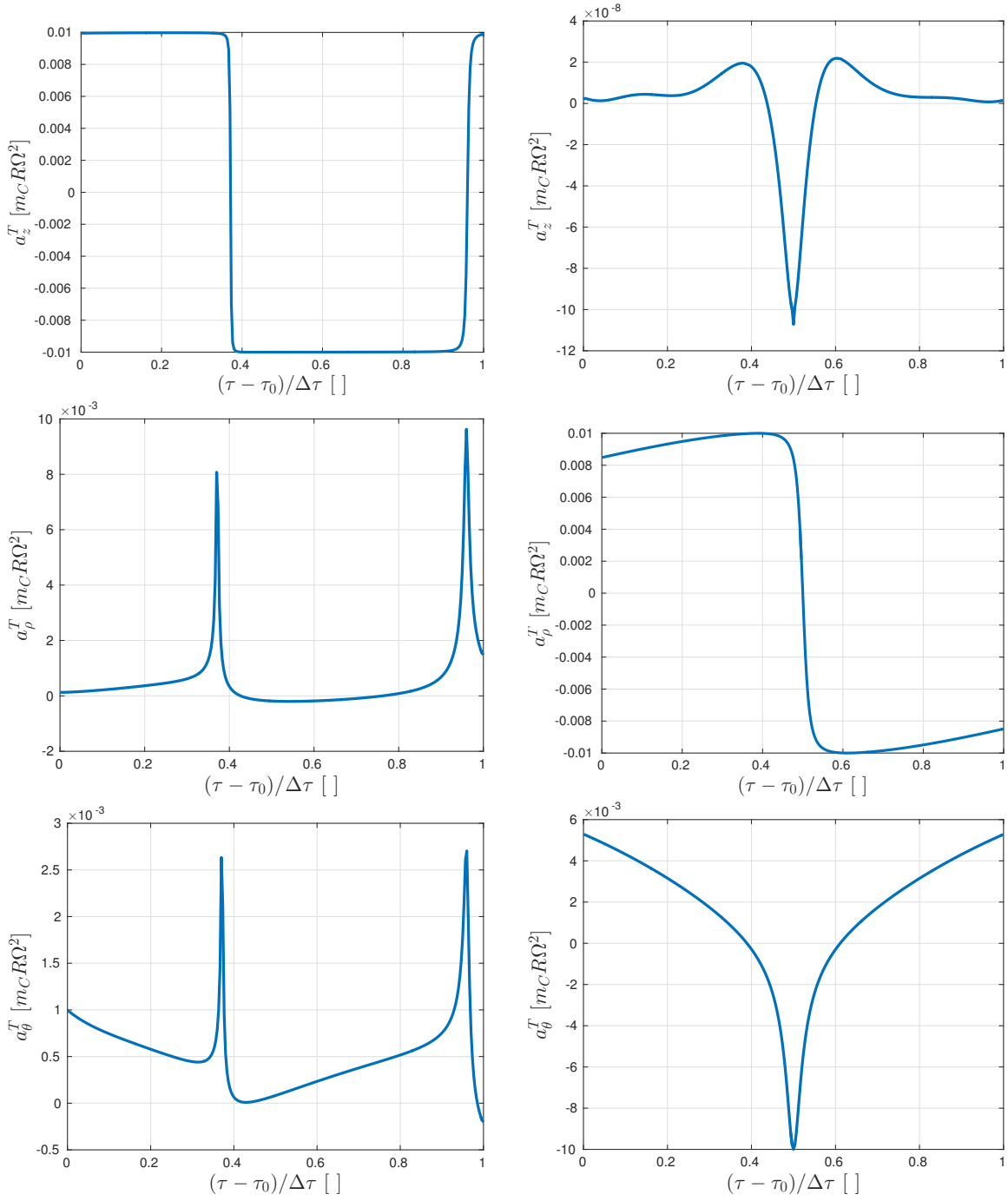


**Figure 5. Thrust profiles for two optimal orbit corrections with  $\varepsilon = 0.01$  and  $\Delta R = 29.7$  km; left figure corresponds to  $\Delta i = 2$  deg and right figure to  $\Delta i = 0$  deg.**

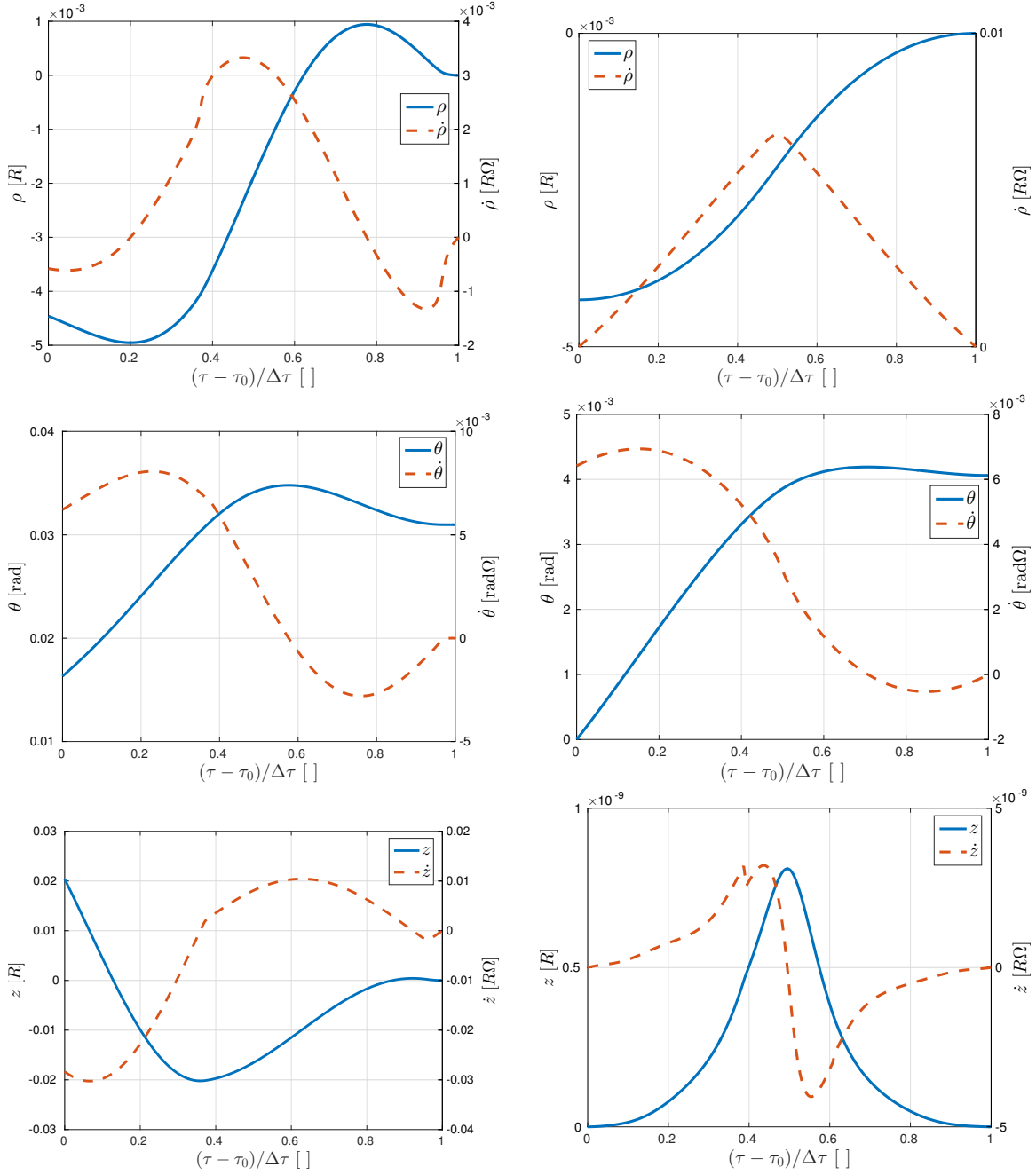


**Figure 6. Radial, angular and out-of-plane curvilinear coordinates and their derivatives for two optimal orbit corrections with  $\varepsilon = 0.01$  and  $\Delta R = 29.7$  km; left figure corresponds to  $\Delta i = 2$  deg and right figure to  $\Delta i = 0$  deg.**

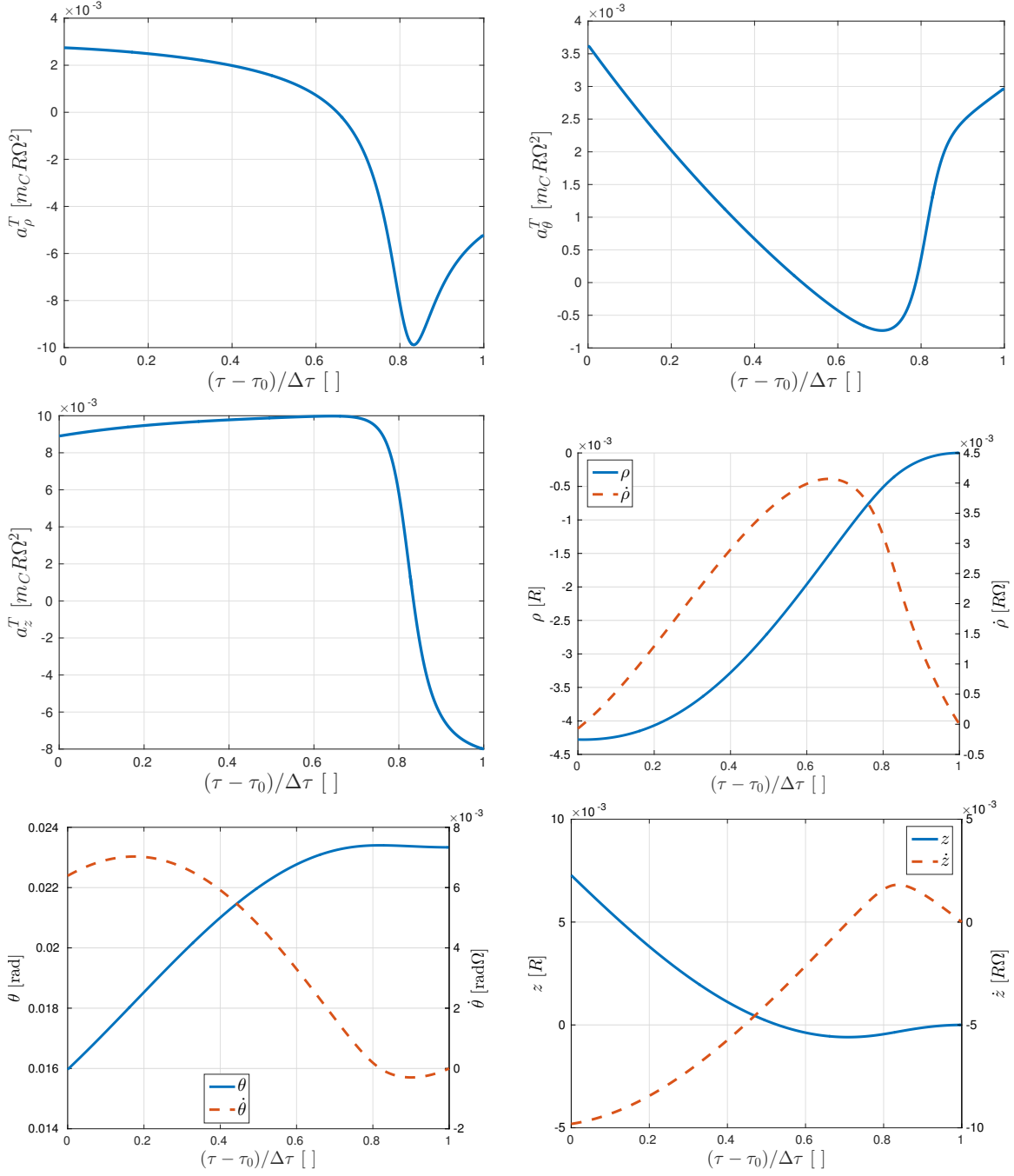


**Figure 7. Thrust control law and state evolution for an orbit correction with  $\varepsilon = 0.01$ ,  $\Delta R = 29.7$  km and  $\Delta i = 0.7$  deg.**

that the curves of  $\Delta\tau$  as a function of  $\Delta i$  for different values of  $\Delta r$  get closer as the inclination change increases. This supports the intuitive idea that the simultaneous change of orbital radius and inclination presents some synergy, with the available thrust being distributed according to which are the more efficient parts of the orbit to modify each element. To quantify this effect, a synergy coefficient  $\sigma$  is proposed as follows:

$$\Delta\tau = \frac{\Delta\tau_r + \Delta\tau_i}{1 + \sigma} \Rightarrow \sigma = \frac{\Delta\tau_r + \Delta\tau_i}{\Delta\tau} - 1, \quad (11)$$

where  $\Delta\tau_r$  is the time needed for the radius-only ( $\Delta i = 0$ ) maneuver and  $\Delta\tau_i$  is the time for the inclination-only ( $\Delta r = 0$ ) maneuver. Logic dictates that  $\sigma$  should lie between 0 and 1. Negative values of  $\sigma$  would indicate that the combined maneuver take more time than performing two dedicated maneuvers for  $\Delta r$  and  $\Delta i$ , while values of  $\sigma$  greater than 1 would lead to the combined maneuver being shorter than the dedicated maneuvers. Figure 4 shows the evolution of  $\sigma$  with  $\Delta i$  and  $\Delta r$  for the considered value of  $\varepsilon$ . It is straightforward to check that  $\sigma$  goes to zero for the inclination-only and radius only maneuvers, while it presents its maximum value for a ridge along the cases where  $\Delta\tau_i$  and  $\Delta\tau_r$  are equal (marked with a black line in the figures). In other words, as the relative weights of the radius and the inclination changes in the total maneuver become more similar, the synergy factor increases.

The maximum  $\sigma$  ridge in the previous plots also serves to separate the radius-dominated cases from the inclination-dominated ones. Figures 5-6 illustrate the differences in the trajectory and control laws for two transfers situated at different sides of said ridge. Both cases correspond to a radial displacement of 29.7 km, but while the first one is coplanar the second includes a 2 degrees inclination change. The out-of-plane thrust profiles, Figure 5, show that the zero-inclination maneuver devotes only a small fraction of the available thrust to inclination modifications, while the high-inclination maneuver clearly resembles the bang-bang structure predicted by the inclination-only analytical solution. The behavior is reversed for the in-plane thrust components  $a_\rho^T$  and  $a_\theta^T$ , also in Figure 5, with  $a_\rho^T$  being dominant compared to the other two for the zero-inclination maneuver. Similar trends are observed in the evolutions of the state, represented in Figure 6. Finally, it is also interesting to consider a case in the maximum  $\sigma$  region. Figures 7 show the minimum-time transfer for  $\Delta R = 29.7$  km and  $\Delta i = 0.7$  deg. Contrary to the previous examples, the available thrust is more evenly distributed between its in-plane and out-of-plane components, although their qualitative behaviors loosely resemble their dominant-case profiles. The variations of the different elements of the state also show comparable orders of magnitude along the transfer.

Moving towards smaller, and more typical, values of the thrust parameter, Figures 9-12 show the times of flight for  $\varepsilon = 0.001$  and  $\varepsilon = 0.0001$  respectively. The same ranges of radial displacement and inclination change studied so far are used for the former, while smaller values of the inclination are considered for the latter. The overall behavior is similar to the  $\varepsilon = 0.01$  case, although the evolution of time with  $\Delta i$  is smoother, without the steep increase shown by that family of maneuvers around  $\Delta i = 1.1$  deg. Furthermore, most of the transfers now take more than one orbit to complete. The synergy coefficient, Figures 11-12, also behaves similarly, with the minimum  $\sigma$  rift displaced towards higher values of the radial displacement. Finally, Figures 8 depict a multi-revolution transfer for  $\varepsilon = 0.001$ ,  $\Delta R = 100$  km and  $\Delta i = 1.0$  deg. Clearly repetitive patterns are observed for the state and control, which show the same structures previously discussed. It is interesting to highlight that the maximum values of the in-plane components of thrust concentrate around the zero-crossings of the nearly-bang-bang out-of-plane thrust profile, illustrating the thrust-distribution strategies which lead to good synergy coefficients (in this case  $\sigma = 0.2609$ ).

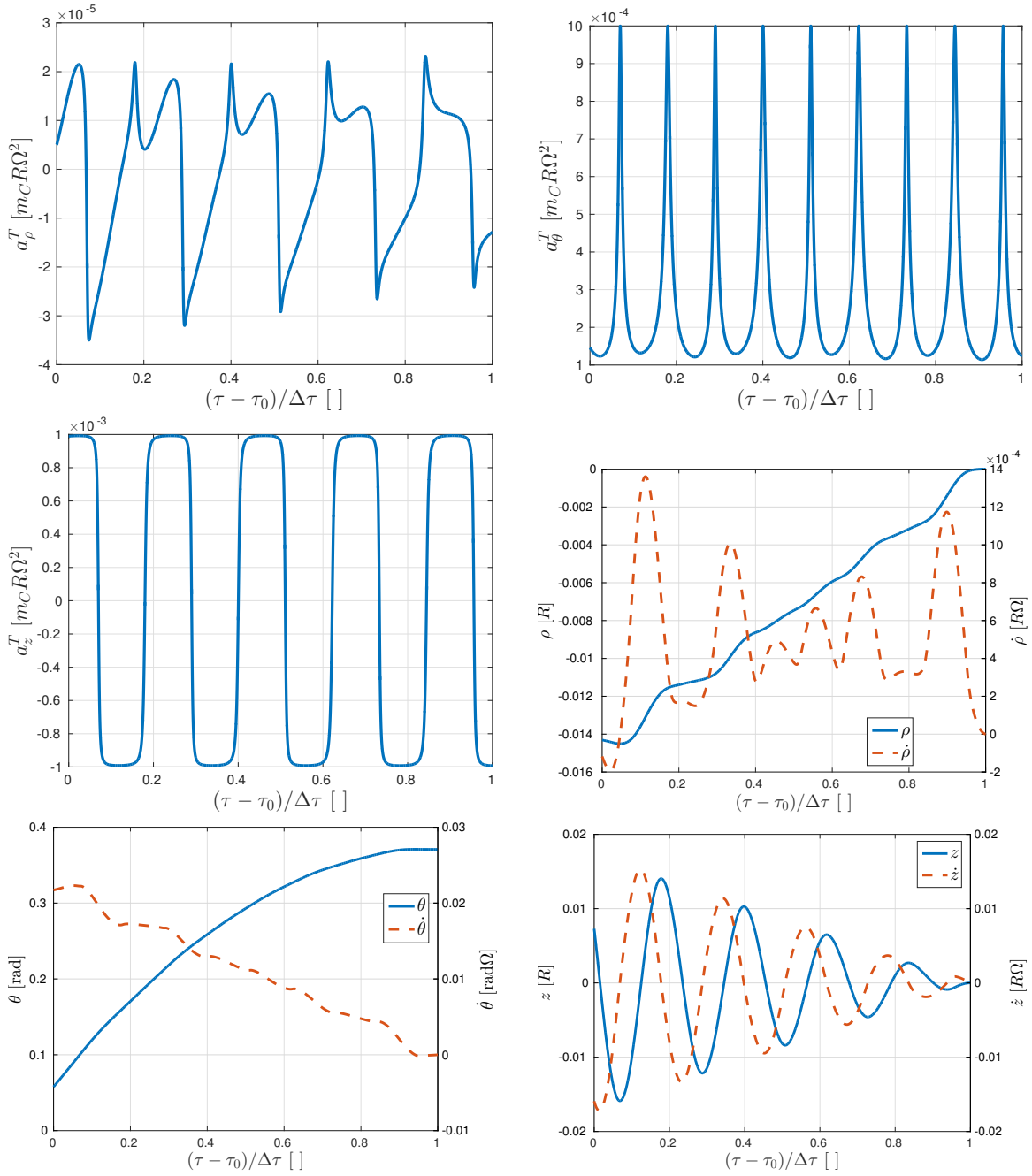


**Figure 8.** Thrust control law and state evolution for an orbit correction with  $\varepsilon = 0.001$ ,  $\Delta R = 100.0$  km and  $\Delta i = 1.0$  deg.

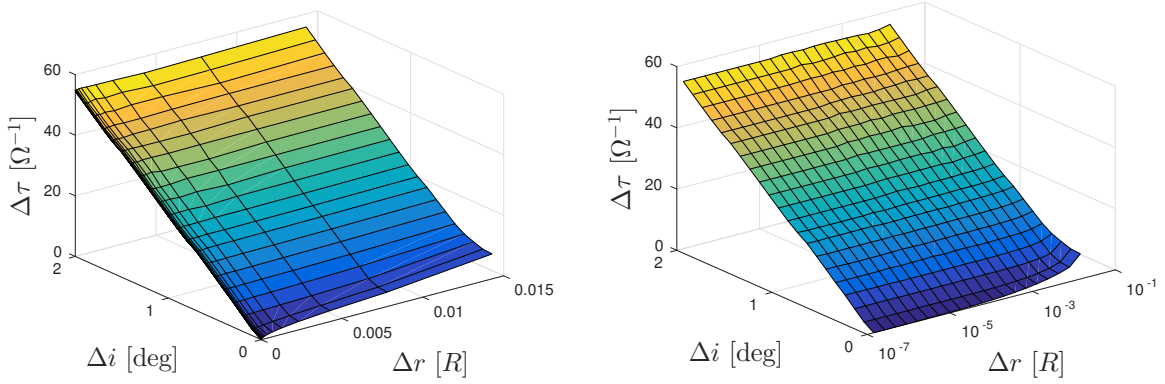


**Figure 9.** Time of flight as a function of the radial displacement and the inclination change for a non-dimensional thrust parameter of 0.001.

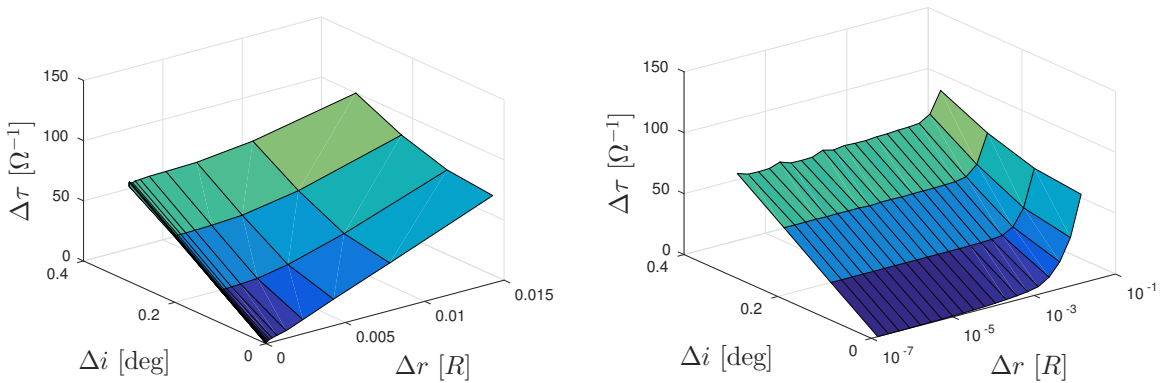


**Figure 10.** Time of flight as a function of the radial displacement and the inclination change for a non-dimensional thrust parameter of 0.0001.

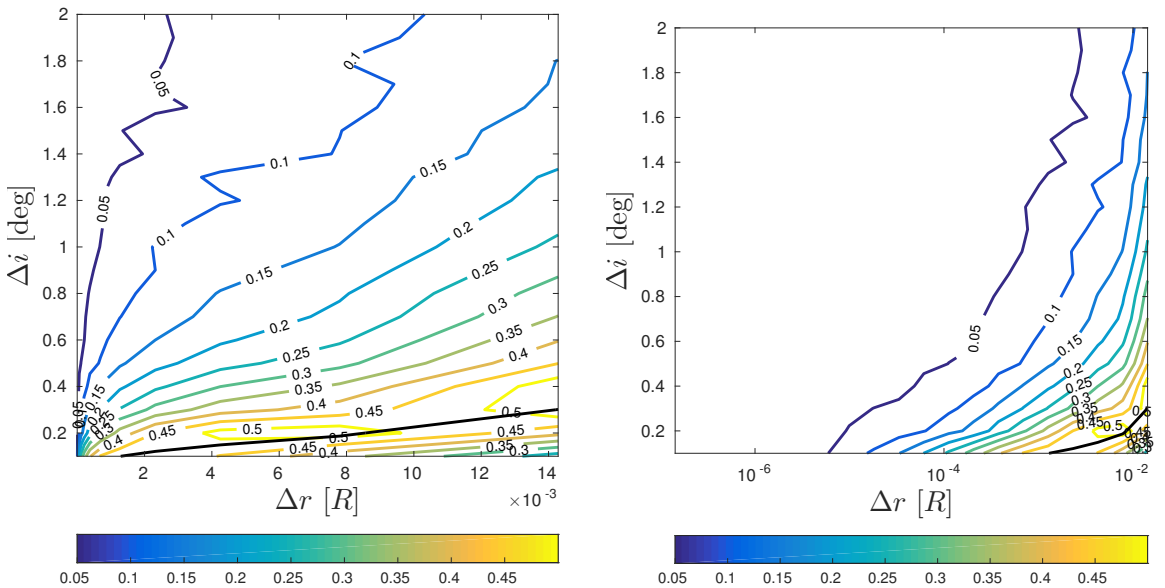


**Figure 11.** Synergy coefficient as a function of the radial displacement and the inclination change for a non-dimensional thrust parameter of 0.001.



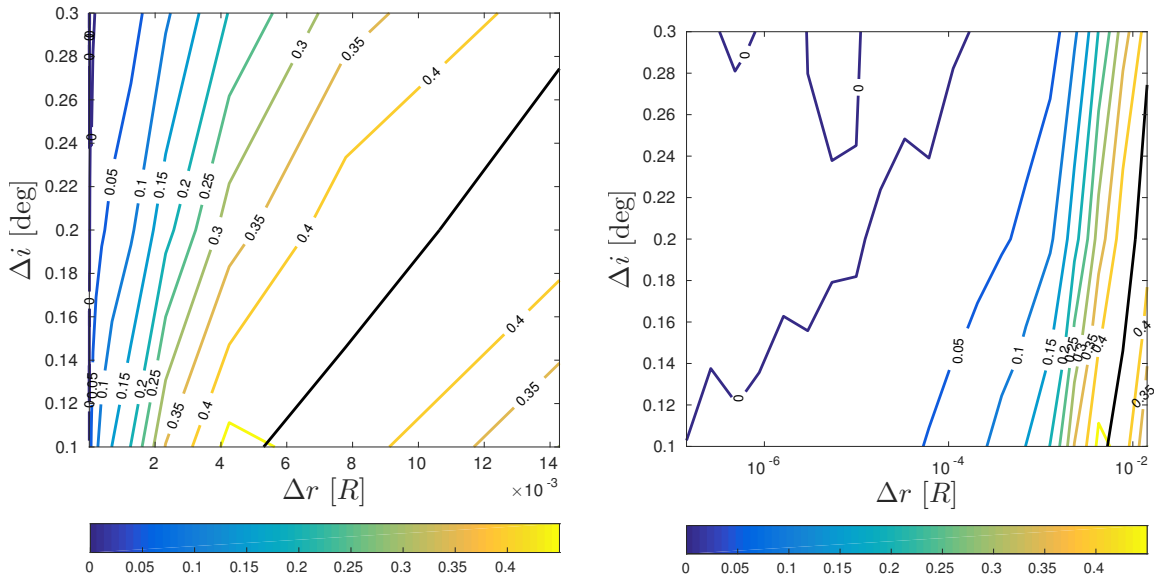


**Figure 12. Synergy factor as a function of the radial displacement and the inclination change for a non-dimensional thrust parameter of 0.0001.**

## CONCLUSION

The minimum-time continuous-thrust orbit correction between two close, non-coplanar, circular orbits has been studied, using a non-linear relative motion formulation in curvilinear coordinates and the direct method. An analytical solution for the minimum-time change of inclination with unaltered orbit radius has been obtained in closed form for the linearized problem, providing an expression of the required maneuver time and qualitative insight about the optimal thrust profile. The ratio of the required inclination change and the available thrust has been identified as the main driver of the maneuver time, and the thrust profile shows a bang-bang structure. These results complement the similar studies already performed by the authors for the phasing and radius change problems. The complete optimal control problem has been numerically solved for several values of inclination and radial displacement, validating the previous time estimates and showing their suitability as initial guesses generators. A synergistic behavior between inclination and radius change has been observed and quantified by comparing the total maneuver time with the sum of the times required for the inclination-only and radius-only maneuvers, showing that this synergy reaches its maximum when the times for the individual maneuvers are equal.

## ACKNOWLEDGMENT

This work has been supported by the Spanish Ministry of Education, Culture and Sport through its FPU Program (reference number FPU13/05910), and by the Spanish Ministry of Economy and Competitiveness within the framework of the research project “Dynamical Analysis, Advanced Orbital Propagation, and Simulation of Complex Space Systems” (ESP2013-41634-P). The authors also want to thank the funding received from the European Union Seventh Framework Programme (FP7/2007-2013) under grant agreement N 607457 (LEOSWEEP).

## REFERENCES

- [1] C. Bombardelli and J. Peláez, “Ion beam shepherd for contactless space debris removal,” *Journal of Guidance, Control, and Dynamics*, Vol. 34, No. 3, 2011, pp. 916–920.
- [2] J. P. Marec, *Optimal space trajectories*, Vol. 1. Elsevier, 2012.
- [3] C. D. Hall and V. Collazo-Perez, “Minimum-time orbital phasing maneuvers,” *Journal of guidance, control, and dynamics*, Vol. 26, No. 6, 2003, pp. 934–941.
- [4] J. L. Gonzalo and C. Bombardelli, “Optimal Low-Thrust-Based Rendezvous Maneuvers,” *Advances in the Astronautical Sciences*, No. AAS 15-364, Williamsburg, Virginia, USA, AAS/AIAA, January 11-15 2015.
- [5] J. L. Gonzalo and C. Bombardelli, “Optimal Low Thrust Orbit Correction in Curvilinear Coordinates,” *Advances in the Astronautical Sciences*, No. AAS 15-695, Vail, Colorado, USA, AAS/AIAA, August 9-13 2015.
- [6] C. Bombardelli, J. L. Gonzalo, and J. Roa, “Compact Solution of Circular Orbit Relative motion in Curvilinear Coordinates,” *Advances in the Astronautical Sciences*, No. AAS 15-661, Vail, Colorado, USA, AAS/AIAA, August 9-13 2015.
- [7] W. Clohessy and R. Wiltshire, “Terminal guidance system for satellite rendezvous,” *Journal of the Aerospace Sciences*, Vol. 27, No. 9, 1960, pp. 653–658. DOI: 10.2514/8.8704.
- [8] J. T. Betts, *Practical Methods for Optimal Control and Estimation Using Nonlinear Programming, Second Edition*. SIAM, 2010.
- [9] F. Topputo and C. Zhang, “Survey of Direct Transcription for Low-Thrust Space Trajectory Optimization with Applications,” *Abstract and Applied Analysis*, Vol. 2014, Hindawi Publishing Corporation, 2014.
- [10] J. L. Gonzalo, “Perturbation Methods in Optimal Control Problems Applied to Low Thrust Space Trajectories,” Master’s thesis, ETSI Aeronáuticos, Technical University of Madrid (UPM), 2012.
- [11] A. Wächter and L. T. Biegler, “On the implementation of an interior-point filter line-search algorithm for large-scale nonlinear programming,” *Mathematical programming*, Vol. 106, No. 1, 2006, pp. 25–57.
- [12] T. F. Coleman, B. S. Garbow, and J. J. Moré, “Software for Estimating Sparse Hessian Matrices,” *ACM Transactions on Mathematical Software*, No. 11, 1985, pp. 363–377.